

NANO EXPRESS

Open Access

Color-tunable up-conversion emission in $\text{Y}_2\text{O}_3:\text{Yb}^{3+}$, Er^{3+} nanoparticles prepared by polymer complex solution method

Vesna M Lojpur¹, Phillip S Ahrenkiel² and Miroslav D Dramićanin^{1*}

Abstract

Powders of Y_2O_3 co-doped with Yb^{3+} and Er^{3+} composed of well-crystallized nanoparticles (30 to 50 nm in diameter) with no adsorbed ligand species on their surface are prepared by polymer complex solution method. These powders exhibit up-conversion emission upon 978-nm excitation with a color that can be tuned from green to red by changing the $\text{Yb}^{3+}/\text{Er}^{3+}$ concentration ratio. The mechanism underlying up-conversion color changes is presented along with material structural and optical properties.

Keywords: Luminescence, Up-conversion, Nanoparticles, Rare earth, Combustion

PACS: 42.70.-a, 78.55.Hx, 78.60.-b

Background

Up-conversion materials have the ability to convert lower energy near-infrared radiations into higher energy visible radiations. These materials have gained considerable attention because of their use in a wide range of important applications, from solid compact laser devices operating in the visible region and infrared quantum counter detectors to three-dimensional displays, temperature sensors, solar cells, anti-counterfeiting, and biological fluorescence labels and probes [1-6]. Further efforts in development of methods for preparation of up-conversion (UC) materials are therefore justified with aims of enhancing their UC efficiency and reducing production costs. In addition, methods for UC nanoparticle (UCNP) synthesis are of particular interest for use in two-photon bio-imaging, sensitive luminescent bio-labels, and GaAs-coated highly efficient light-emitting diodes [7].

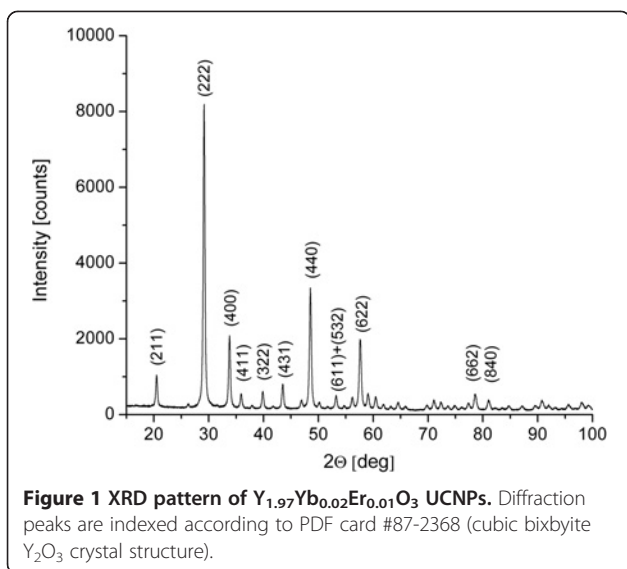
Lanthanide-based UC materials and UCNPs are of special interest due to unique spectroscopic properties of rare-earth ions like sharp intra- $4f$ electronic transitions and existence of abundant, long-living electronic excited states at various energies that facilitate electron promotion to high-energy states [8]. In principal, lanthanide-based

UC materials and UCNPs consist of three components: a host matrix, a sensitizer, and an activator dopant. The choice of the host lattice determines the distance between the dopant ions, their relative spatial position, their coordination numbers, and the type of anions surrounding the dopant. The properties of the host lattice and its interaction with the dopant ions therefore have a strong influence on the UC process [9]. It has been shown that UC emission efficiency depends strongly on host phonon energy, where in low-phonon-energy hosts, multi-phonon relaxation processes are depressed and efficiency-enhanced [10]. Because of their excellent chemical stability, broad transparency range, and good thermal conductivity, rare-earth sesquioxides are well-suited host materials [11]. Their phonon energy (*ca.* 560 cm^{-1}) is higher compared to the most UC-efficient fluoride materials (*ca.* 350 cm^{-1}), but lower compared to other host types (phosphates, vanadates, molybdates, titanates, zirconates, silicates, etc.). In addition, easy doping can be achieved with RE ions because of similarity in ionic radius and charge. For sensitizer dopant, Yb^{3+} is the most common choice for excitation around 980 nm, where a variety of inexpensive optical sources exists. This ion has a simple energy level structure with two levels and a larger absorption cross section compared to other trivalent rare-earth ions. The energy separation of Yb^{3+} $^2\text{F}_{7/2}$ ground state and $^2\text{F}_{5/2}$ excited state match-up well the transitions of an activator dopant ion, which has

* Correspondence: dramican@vinca.rs

¹Vinča Institute of Nuclear Sciences, University of Belgrade, P.O. Box 522, Belgrade 11001, Serbia

Full list of author information is available at the end of the article



easy charge transfer between its excited state and activator states. For visible emission, Er^{3+} , Tm^{3+} , Ho^{3+} , and Pr^{3+} are commonly used as activator dopants [12-16]. UC emission of different colors can be obtained in a material with different activators and their combinations. Er^{3+} -doped materials emit green and red light, Tm^{3+} blue, Ho^{3+} green, and Pr^{3+} red.

In recent times, a lot of effort is directed towards UC color tuning to obtain a material with characteristic emission usually by combining two or more activator ions [17] or by utilizing electron–electron and electron–phonon interactions in existing one-activator systems [18,19]. In this research we showed that color tuning from green to red can be achieved in Yb^{3+}/Er^{3+} UCNP systems on account of changes of Yb^{3+} sensitizer concentration. For this purpose we prepared Y_2O_3 NPs, the most well-known rare-earth sesquioxide host, co-doped with different Yb^{3+}/Er^{3+} ratios. Nanosized phosphors offer a number of potential advantages over traditional, micro-scale ones in optical properties, such as high-resolution images and high luminescence efficiency

[20,21]. However, Vetrone et al. showed that CO_3^{2-} and OH^- species are frequently adsorbed on the surface of sesquioxide nanoparticles [22]. Their high vibrational energies (about 1,500 and 3,350 cm^{-1} for CO_3^{2-} and OH^- , respectively) decrease the UC efficiency through multi-phonon relaxations. For this reason we applied polymer complex solution (PCS) synthesis [23] since we found earlier that the PCS method provides sesquioxides with low surface area and defects and no adsorbed species on the surface [24-26].

Methods

Sample fabrication

Polymer complex solution method is a modified combustion method where instead of classical fuel (urea, glycine, carbonylhydrazide) an organic water-soluble polymer (in our case polyethylene glycol (PEG)) is used. The utility of this polymeric approach comes from the coordination of metal cations on the polymer chains during gelation process, resulting in very low cation mobility. Polymer precursor works both as a chelating agent and as an organic fuel to provide combustion heat for the calcination process. In this way PCS provides mixing of constituting elements at the atomic level and allows homogeneous control of very small dopant concentration. The first step in the PCS method is preparation of an aqueous solution containing metal salts and PEG. In the second step, removal of the excess water forces polymer species into closer proximity, converting the system into a resin-like gel. Upon ignition, an oxide powder is obtained, while considerable resin mass is lost as the polymer matrix is burned away.

Using this procedure, three Y_2O_3 samples doped with 0.5 at.% of Er^{3+} and 1, 2.5, and 5 at.% of Yb^{3+} ions were synthesized. In brief, appropriate stoichiometric quantities of yttrium oxide (Y_2O_3), erbium oxide (Er_2O_3), and ytterbium oxide (Yb_2O_3) (all Alfa Aesar, 99.9%, Ward Hill, MA, USA) were mixed and dissolved in hot nitric acid. In the obtained solutions, PEG ($M_w = 200$, Alfa Aesar) was added in 1:1 mass ratio. The formed

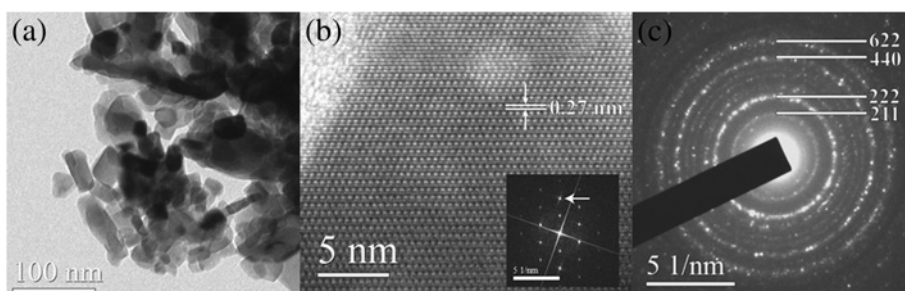
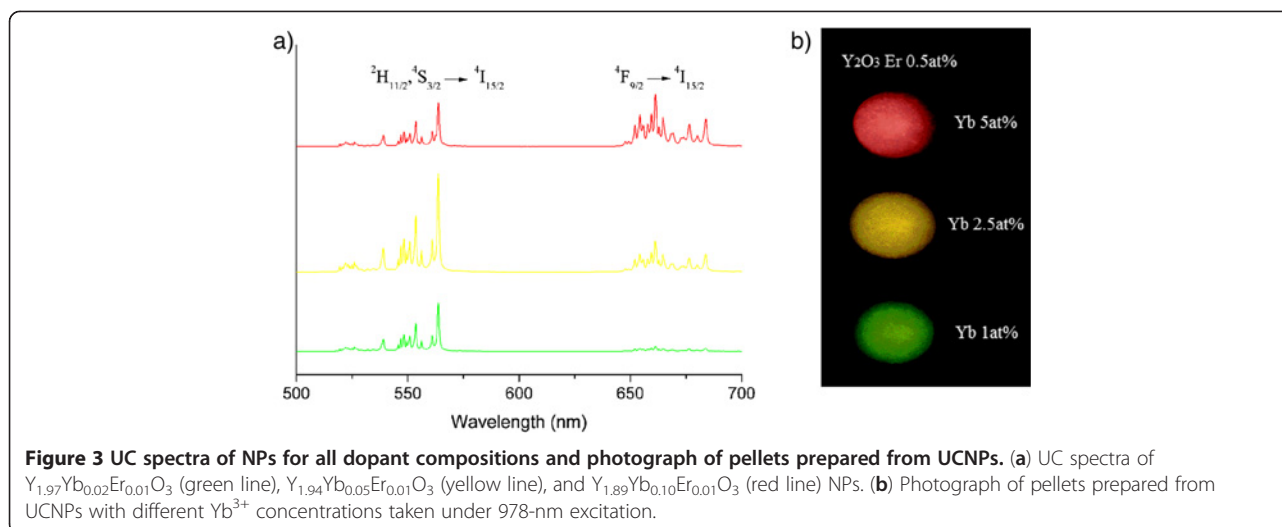


Figure 2 TEM data from $Y_{1.97}Yb_{0.02}Er_{0.01}O_3$ sample. (a) Bright-field image showing nanoparticle cluster. (b) [110] lattice image of a single particle. The 004 planes are indicated. Inset: FFT of image (indicated spot corresponds to 004 periodicity). (c) Selected-area diffraction pattern of nanoparticle cluster. Prominent planes are indexed.



metal-PEG solution was stirred at 80°C, resulting in a metal-PEG solid complex which was further fired at 800°C in air. The powders were additionally annealed at 800°C for 2 h in order to decompose the residual PEG and nitrite ions and to obtain pure crystal phase.

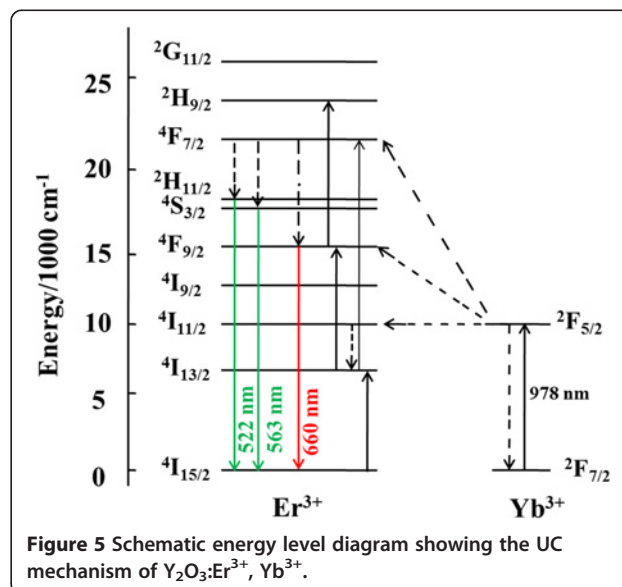
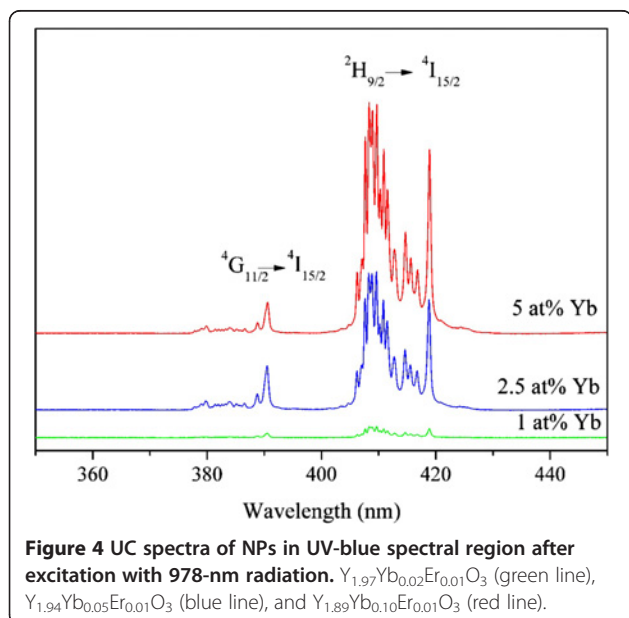
Characterization methods

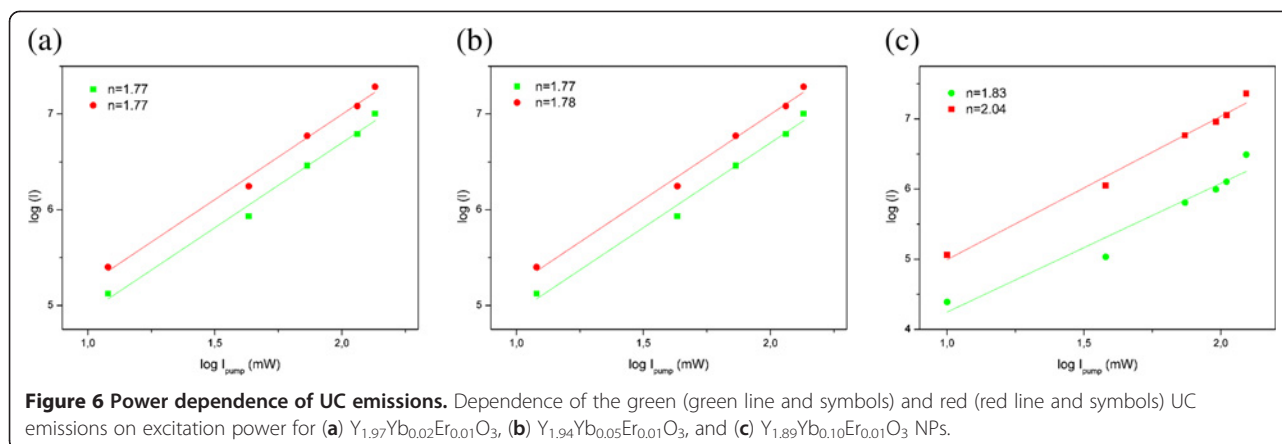
Crystal structures of samples are checked by X-ray diffraction (XRD) measurements. Measurements are performed on a Rigaku SmartLab system (Shibuya-ku, Japan) operating with Cu $K\alpha_{1,2}$ radiation at 30 mA and 40 kV, in the 2θ range from 15° to 100° (using continuous scan of 0.7°/s). Transmission electron microscopy (TEM) is conducted using a JEOL-JEM 2100 instrument (Akishima-shi, Japan) equipped with LaB₆ cathode and operated at 200 kV.

The up-conversion luminescence emissions and decays are measured upon excitation with 978-nm radiation (OPO EKSPLA NT 342, 5.2-ns pulse, Vilnius, Lithuania) on a Horiba Jobin-Yvon Model FHR1000 spectrofluorometer system (Kyoto, Japan) equipped with an ICCD Jobin-Yvon 3771 detector. For measurements of up-conversion emission intensity dependence on excitation power, a continuous-wave laser is used (980-nm radiation).

Results and discussion

The representative XRD pattern for the $Y_{1.97}Yb_{0.02}Er_{0.01}O_3$ -doped sample is shown in Figure 1. The XRD analysis confirms the presence of a cubic bixbyite Y_2O_3 crystal structure with space group $Ia-3$ (no. 206), with diffraction peaks indexed according to the PDF card #87-2368. No other phases were detected and the small peak shifts in





respect to pure Y_2O_3 are observed, indicating that Er^{3+} and Yb^{3+} ions have been effectively incorporated into the host lattice. An average crystallite size in the range of 21 nm is found by Halder-Wagner method analysis of all major diffraction peaks.

The presence of nitrate, water, and carbon species on nanoparticle surfaces is checked by Fourier transform infrared (FT-IR) spectroscopy. Only Y-O stretching vibrations of the host lattice at 560 cm^{-1} are noted (see Additional file 1: Figure S1 for the FT-IR spectrum of $\text{Y}_{1.97}\text{Yb}_{0.02}\text{Er}_{0.01}\text{O}_3$ sample). This is favorable for efficient emission since the high phonon energy of species adsorbed on the surface of nanoparticles may enhance significantly nonradiative de-excitation [13,22].

The UCNPs are further investigated by transmission electron microscopy, and representative images are given in Figure 2. One can see highly agglomerated crystalline nanoparticles with irregular, polygonal-like shapes having a size in the range of 30 to 50 nm with boundary lines observed clearly in some regions (Figure 2a). Strong particle agglomeration is a main drawback of the PCS synthesis method. It is a consequence of an extremely high temperature gradient that occurs while firing metal-PEG complex. At that instance a large amount of high-pressure vapors is produced in the sample that strongly press particles onto each other. On the other hand, high-temperature gradients and pressure facilitate production of well-crystallized powder. An examination at higher magnifications (Figure 2b) reveals that grain boundaries are without any irregularities and that the surface of observed crystals is free of defects and without any amorphous layers. The spotty ring selected-area electron diffraction pattern (Figure 2c) confirms that Y_2O_3 powder is polycrystalline and is related to the fact that the constituent crystallites have a size of about 20 nm.

The up-conversion luminescence spectra of NPs, for all Yb/Er dopant compositions, are measured upon excitation with 978-nm radiation. The main red and green emissions are shown in Figure 3a. They

originate from Er^{3+} $f-f$ electronic transitions $^4\text{F}_{9/2} \rightarrow ^4\text{I}_{15/2}$ (red emission) and $(^2\text{H}_{11/2}, ^4\text{S}_{3/2}) \rightarrow ^4\text{I}_{15/2}$ (green emission) and are facilitated by the two-photon UC process. Weak emissions from higher photon order UC processes can be observed in the blue spectral (410 nm, $^2\text{H}_{9/2} \rightarrow ^4\text{I}_{15/2}$ transition) and UV (390 nm, $^4\text{G}_{11/2} \rightarrow ^4\text{I}_{15/2}$ transition) regions shown in Figure 4. These higher photon order emission diminishes in NPs with lower Yb^{3+} content ($\text{Y}_{1.97}\text{Yb}_{0.02}\text{Er}_{0.01}\text{O}_3$). The variation in Yb^{3+} concentration alters the red-to-green emission ratio (see Figure 3a), and consequently overall UC color of NPs is changed (see Figure 3b). The highest Yb^{3+} concentration of 5 at.% produces red color, and yellow is obtained with 2.5 at.% and green with 1 at.%.

The energy level diagram of Yb^{3+} and Er^{3+} is shown in Figure 5 and illustrates the energy transfer from Yb^{3+} to Er^{3+} which generates up-conversion in a following manner: population of $^4\text{F}_{7/2}$ level in Er^{3+} leads to an intermediate non-radiative relaxation to the $^2\text{H}_{11/2}$ and $^4\text{S}_{3/2}$ levels and further to two partially overlapped green emissions at 522 and 563 nm due to the radiative relaxations to the $^4\text{I}_{15/2}$ level. Alternatively, the $^4\text{F}_{7/2}$ level can partially non-radiatively relax to the $^4\text{F}_{9/2}$ level from which red emission at 660 nm originates ($^4\text{F}_{9/2} \rightarrow ^4\text{I}_{15/2}$). Red emission could be intensified by another up-conversion path which occurs after non-radiative relaxation of the $^4\text{I}_{11/2}$ to the $^4\text{I}_{13/2}$ level, from where the additional population of the $^4\text{F}_{9/2}$ level occurs through energy transfer.

Table 1 Emission decay times for $\text{Y}_2\text{O}_3:\text{Yb}^{3+}$, Er^{3+} nanoparticles upon 978-nm excitation

	Green emission lifetime (ms)	Red emission lifetime (ms)
$\text{Y}_{1.97}\text{Yb}_{0.02}\text{Er}_{0.01}\text{O}_3$	0.36	0.71
$\text{Y}_{1.94}\text{Yb}_{0.05}\text{Er}_{0.01}\text{O}_3$	0.38	0.60
$\text{Y}_{1.89}\text{Yb}_{0.10}\text{Er}_{0.01}\text{O}_3$	0.34	0.35

The population of the $^2H_{9/2}$ level is realized by the excited state absorption from $^4I_{13/2}$ and $^4F_{9/2}$ levels. Blue up-conversion emission occurs by its radiative de-excitations to the $^4I_{15/2}$ level. Power dependence of UC emissions, given in Figure 6, confirms that two-photon processes are responsible for green and red UC emissions. The observed slopes are similar for 1 and 2.5 at.% Yb^{3+} -doped samples and slightly higher for 5 at.% Yb^{3+} doping.

Changes in red-to-green emission ratio with Yb^{3+} concentration increase in $Y_2O_3:Er^{3+}$ bulk and NPs are discussed by Vetrone et al. [22]. They observed this phenomenon to be much more pronounced in NPs compared to bulk. They concluded that a cross-relaxation mechanism of $^4F_{7/2} \rightarrow ^4F_{9/2}$ and $^4F_{9/2} \leftarrow ^4I_{11/2}$ is partly responsible for the red enhancement, but phonons of ligand species present on the NP surface enhance the probability of $^4F_{9/2}$ level population from the $^4I_{13/2}$ level. However, in the present case, no adsorbed species on the NPs are detected, as in other cases of NPs prepared with the PCS method. TEM images in Figure 2 and the Stark splitting of emission clearly evident in Figure 3a demonstrate the crystalline nature of NPs. Also, the values of UC emission decays, given in Table 1, are much larger compared to those from [22], indicating in this way the absence of a strong ligand influence on UC processes. Silver et al. [27] noticed that the $Yb^{3+} \ ^2F_{5/2}$ excited level may also receive electrons from higher energy levels of nearby Er^{3+} ions, back transferring energy from Er^{3+} to Yb^{3+} ions. When they compared spectra of $Y_2O_3:Eu^{3+}$ with Yb^{3+} , they noted that the up-conversion and down-conversion emissions lost intensity in the presence of Yb^{3+} and that was least apparent for the red $^4F_{9/2} \rightarrow ^4I_{15/2}$ transition, even for a Yb^{3+}/Er^{3+} ratio of 5:0.5. The decrease of $^4F_{9/2}$ lifetime with Yb^{3+} concentration increase (Table 1) is a consequence of enlarged population of $^2H_{9/2}$ by excited state absorption from the $^4F_{9/2}$ level, which is evidenced through enhancement of blue emission ($^2H_{9/2} \rightarrow ^4I_{15/2}$) for larger Yb^{3+} content (see Figure 4).

Conclusions

In conclusion, yttrium oxide powders doped with Er^{3+} ions and co-doped with different concentrations of Yb^{3+} ions are successfully prepared using polymer complex solution method. This simple and fast synthesis method provides powders consisting of well-crystallized nanoparticles (30 to 50 nm in diameter) with no adsorbed species on their surface. The powders exhibit up-conversion emission upon 978-nm excitation, with a color that can be tuned from green to red by changing the Yb^{3+}/Er^{3+} concentration ratio. This effect can be achieved in nanostructured hosts where electron-phonon interaction is altered compared to the bulk material.

Additional file

Additional file 1: Figure S1. FT-IR spectrum of $Y_{1.97}Yb_{0.02}Er_{0.01}O_3$.

Competing interests

The authors declare that they have no competing interests.

Authors' contributions

VL carried out the material synthesis. PA performed the TEM study. VL and MD carried out the X-ray diffraction and luminescence analysis. MD supervised the research activity. VL and MD wrote the manuscript. All authors discussed and commented on the manuscript. All authors approved the final manuscript.

Acknowledgments

The authors would like to acknowledge the support from the Ministry of Education, Science and Technological Development of the Republic of Serbia (grant no. 45020).

Author details

¹Vinča Institute of Nuclear Sciences, University of Belgrade, P.O. Box 522, Belgrade 11001, Serbia. ²South Dakota School of Mines & Technology, Rapid City, SD 57701, USA.

Received: 10 February 2013 Accepted: 11 March 2013

Published: 22 March 2013

References

- Vetrone F, Boyer JC, Capobianco JA, Speghini A, Bettinelli M: **980 nm excited upconversion in an Er-doped ZnO-TeO₂ glass.** *Appl Phys Lett* 2002, **80**(10):1752–1754.
- Man SQ, Pun EYB, Chung PS: **Upconversion luminescence of Er³⁺ in alkali bismuth gallate glasses.** *Appl Phys Lett* 2000, **77**(4):483–485.
- Zhang HX, Kam CH, Zhou Y, Han XQ, Buddhudu S, Xiang Q, Lam YL, Chan YC: **Green upconversion luminescence in Er³⁺:BaTiO₃ films.** *Appl Phys Lett* 2000, **77**(5):609–611.
- Luo XX, Cao WH: **Upconversion luminescence of holmium and ytterbium co-doped yttrium oxysulfide phosphor.** *Mater Lett* 2007, **61**(17):3696–3700.
- Zhan J, Shen H, Guo W, Wang S, Zhu C, Xue F, Hou J, Su H, Yuan Z: **An upconversion NaYF₄:Yb³⁺, Er³⁺/TiO₂ core-shell nanoparticle photoelectrode for improved efficiencies of dye-sensitized solar cells.** *J Power Sources* 2013, **226**:47–53.
- Ming C, Song F, Ren X: **Color variety of up-conversion emission of Er³⁺/Yb³⁺ co-doped phosphate glass ceramics.** *Curr Appl Phys* 2013, **13**(2):351–354.
- Liu G, Chen X: **Spectroscopic properties of lanthanides in nanomaterials.** In *Handbook on the Physics and Chemistry of Rare Earths*. Edited by Gschneide KA Jr, Bünzli J-CG, Pecharsky VK. Amsterdam: Elsevier; 2007:99–169.
- Sivakumar S, van Veggel FCJM, May PS: **Near-infrared (NIR) to red and green up-conversion emission from silica sol-gel thin films made with La_{0.45}Yb_{0.50}Er_{0.05}F₃ nanoparticles, hetero-looping-enhanced energy transfer (Hetero-LEET): a new up-conversion process.** *J Am Chem Soc* 2007, **129**(3):620–625.
- Haase M, Schäfer H: **Upconverting nanoparticles.** *Angew Chem Int Edit* 2011, **50**(26):5808–5829.
- Zhang T, Yu L, Wang J, Wu J: **Microstructure and up-conversion luminescence of Yb³⁺ and Ho³⁺ co-doped BST tick films.** *J Mater Sci* 2010, **45**(24):6819–6823.
- Martinez A, Morales J, Diaz-Torres LA, Salas P, De la Rosa E, Oliva J, Desirena H: **Green and red upconverted emission of hydrothermal synthesized Y₂O₃:Er³⁺-Yb³⁺ nanophosphors using different solvent ratio conditions.** *Mater Sci Eng B* 2010, **174**(1–3):164–168.
- Yang Z, Yan L, Yan D, Song Z, Zhou D, Jin Z, Qui J: **Color tunable upconversion emission in Yb, Er co-doped bismuth titanate inverse opal.** *J Am Chem Soc* 2011, **94**(8):2308–2310.
- Capobianco JA, Boyer JC, Vetrone F, Speghini A, Bettinelli M: **Optical spectroscopy and upconversion studies of Ho³⁺-doped bulk and nanocrystalline Y₂O₃.** *Chem Mater* 2002, **14**(7):2915–2921.
- Guyot Y, Moncorge R, Merkle LF, Pinto A, McIntosh B, Verdun H: **Luminescence properties of Y₂O₃ single crystals doped with Pr³⁺ or Tm³⁺ and codoped with Yb³⁺, Tb³⁺ or Ho³⁺ ions.** *Opt Mater* 1996, **5**(1–2):127–136.

15. Wang X, Bu Y, Xiao S, Yang X, Ding JW: **Upconversion in Ho^{3+} -doped YbF_3 particle prepared by coprecipitation method.** *J Appl Phys B* 2008, **93**(4):801–807.
16. Chen GY, Yang GH, Aghahadi B, Liang HJ, Liu Y, Li L, Zhang ZG: **Ultraviolet-blue upconversion emissions of Ho^{3+} ions.** *J Opt Soc Am B* 2010, **27**(6):1158–1164.
17. Gong L, Maa M, Xu C, Li X, Wang S, Lin J, Yang Q: **Multicolor upconversion emission of dispersed ultra small cubic Sr_2LuF_7 nanocrystals synthesized by a solvothermal process.** *J Lumin* 2013, **134**:718–723.
18. Chen Z, Gong W, Chen T, Li S, Wang D, Wang Q: **Preparation and upconversion luminescence of $\text{Er}^{3+}/\text{Yb}^{3+}$ codoped $\text{Y}_2\text{Ti}_2\text{O}_7$ nanocrystals.** *Mater Lett* 2012, **68**:137–139.
19. Xie M, Peng X, Fu X, Zhang J, Li G, Yu X: **Synthesis of $\text{Yb}^{3+}/\text{Er}^{3+}$ co-doped MnF_2 nanocrystals with bright red up-converted fluorescence.** *Scripta Mater* 2009, **60**(3):190–193.
20. Ye X, Zhuang W, Hu Y, He T, Huang X, Liao C, Zhong S, Xu Z, Nie H, Deng G: **Preparation, characterization, and optical properties of nano- and submicron-sized $\text{Y}_2\text{O}_3:\text{Eu}^{3+}$ phosphors.** *J Appl Phys* 2009, **105**(5):064302–064308.
21. Medintz IL, Uyeda HT, Goldman ER, Mattoussi H: **Quantum dot bioconjugates for imaging, labelling and sensing.** *Nat Mater* 2005, **4**(6):435–446.
22. Vetrone F, Boyer JC, Capobianco JA, Spgehini A, Bettinelli M: **Significance of Yb^{3+} concentration on the upconversion mechanisms in codoped $\text{Y}_2\text{O}_3:\text{Er}^{3+}, \text{Yb}^{3+}$ nanocrystals.** *J Appl Phys* 2004, **96**(1):661–667.
23. Lukić SR, Petrović DM, Dramićanin MD, Mitrić M, Djaćanin L: **Optical and structural properties of $\text{Zn}_2\text{SiO}_4:\text{Mn}^{2+}$ green phosphor nanoparticles obtained by a polymer-assisted sol–gel method.** *Scripta Mater* 2008, **58**(8):655–658.
24. Andrić Ž, Dramićanin MD, Mitrić M, Jokanović V, Bessière A, Viana B: **Polymer complex solution synthesis of $(\text{Y}_x\text{Gd}_{1-x})_2\text{O}_3:\text{Eu}^{3+}$ nanopowders.** *Opt Mater* 2008, **30**(7):1023–1027.
25. Antić Ž, Krsmanović R, Wojtowicz M, Zych E, Bártoová B, Dramićanin MD: **Preparation, structural and spectroscopic studies of $(\text{Y}_x\text{Lu}_{1-x})_2\text{O}_3:\text{Eu}^{3+}$ nanopowders.** *Opt Mater* 2010, **32**(12):1612–1617.
26. Krsmanović R, Antić Ž, Bártoová B, Dramićanin MD: **Characterization of rare-earth doped Lu_2O_3 nanopowders prepared with polymer complex solution synthesis.** *J Alloy Compd* 2010, **505**(1):224–228.
27. Silver J, Martinez-Rubio MI, Ireland TG, Fern GR, Withnall R: **The effect of particle morphology and crystallite size on the upconversion luminescence properties of erbium and ytterbium co-doped yttrium oxide phosphors.** *J Phys Chem B* 2001, **105**(5):948–953.

doi:10.1186/1556-276X-8-131

Cite this article as: Lojpur et al.: Color-tunable up-conversion emission in $\text{Y}_2\text{O}_3:\text{Yb}^{3+}, \text{Er}^{3+}$ nanoparticles prepared by polymer complex solution method. *Nanoscale Research Letters* 2013 **8**:131.

Submit your manuscript to a SpringerOpen[®] journal and benefit from:

- Convenient online submission
- Rigorous peer review
- Immediate publication on acceptance
- Open access: articles freely available online
- High visibility within the field
- Retaining the copyright to your article

Submit your next manuscript at ► springeropen.com